香港天文台
HONG KONG OBSERVATORY

Reprint 780

Thunderstorm Downburst and Radar-based Nowcasting of Squalls

Linus H.Y. Yeung, Edwin S.T. Lai and Philip K.Y. Chan

Fifth European Conference on Radar in Meteorology and Hydrology, Helsinki, Finland 30 June - 4 July 2008

Thunderstorm Downburst and Radar-based Nowcasting of Squalls

Linus H.Y. Yeung, Edwin S.T. Lai and Philip K.Y. Chan
Hong Kong Observatory

1. Introduction

Under favourable atmospheric conditions, downdrafts in severe thunderstorms can intensify into downbursts and trigger damaging gust winds or squalls upon impinging the ground. At the Hong Kong Observatory, severe gusts or squalls are defined operationally as 1-sec wind speed reaching 70 km/h (~19.44 m/s) or higher. According to records from 1987 to 2006, the occurrence frequency of severe squalls associated with thunderstorms (tropical cyclone rainbands excluded) in Hong Kong is about 11 days per year on average. Although not as frequent as thunderstorm lightning, such a base rate is actually higher than that of intense rainstorms (50 mm/h or higher) and other rain-related hazards, including landslide and flooding in Hong Kong. As such, the overall impact of severe squalls to the society should not be underestimated. Effective monitoring and predictive tools for mitigating such kind of transient yet high-impact weather hazards are essential.

Based on earlier studies by Squires [1] and Emanuel [2] on the "cloud top penetrative downdraft" mechanism, Stewart [3] developed a wind gust prediction scheme for pulse-type thunderstorms using radar data. An alternative mechanism based on the cooling of air parcel by raindrops evaporation was also put forward, leading to various gust estimation methods [4]-[9]. Following a similar approach, a real-time nowcasting scheme based on radar reflectivity and upper-air sounding data was developed at the Observatory for predicting wet downburst and its consequential squalls. The rationale behind the scheme, a simple conceptual model for convective downdraft physics, is introduced in Section 2. The key processes in the estimation of the three main contributors to squalls are presented in Section 3. In Section 4, development details in the nowcasting algorithm are given. Real-time nowcast performance is presented in Sections 5. In Section 6, limitations and sources of error are discussed. Finally, Section 7 provides the concluding remarks and suggestions on the ways forward.

2. Thunderstorm Downburst Conceptual Model

A convective downdraft was modeled as an air parcel, with initial momentum v_H, linked to three forces in the vertical, namely perturbation pressure gradient force, buoyancy force and precipitation loading (Fig. 1). Following Doswell [10], the pressure gradient force was neglected as it has significant effect only on the updraft in supercells. With this assumption and other simplifications (e.g. requiring the environment of the air parcel to be static on the time scale of the downdraft), the resulting momentum equation is integrated over height to yield the kinetic energy of the parcel on descending to the surface in the following form:

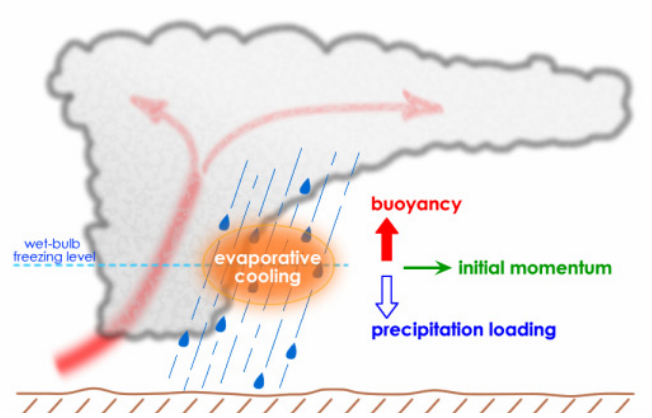

Fig. 1 Schematic diagram illustrating the conceptual model of convective downdraft due to raindrops evaporative cooling of air parcel in the rain shaft.

$$v_s^2 = v_H^2 + U_{\mathrm{BUOY}} + U_{\mathrm{LOAD}} \qquad (1)$$

where the subscripts s and H refer respectively to the surface and the initial altitude where the parcel started to descend. The three terms on the right hand side correspond respectively to the initial kinetic energy of the air parcel at height H, downdraft convective available potential energy (DCAPE) due to negative buoyancy, and gravitational potential energy gained through precipitation loading effect. For more derivation details, interested readers are referred to the work done by Holleman [11].

A downdraft is said to occur if the net force acting on the air parcel is pointing downward, i.e. its overall potential energy is positive:

$$U_{\mathrm{BUOY}} + U_{\mathrm{LOAD}} > 0 \qquad (2)$$

The maximum possible convective gust v_S achievable at the surface is then obtained by taking the square root of Eq.(1). Note that U_{BUOY} could be negative if the buoyancy force is pointing upward, but downdraft is still physically feasible if the precipitation loading is heavy enough such that $|U_{\mathrm{LOAD}}| > |U_{\mathrm{BUOY}}|$. It is assumed that all three sources of energy contribute to the kinetic energy of gust winds at the surface. Section 4.4 below discusses the validity of such an assumption.

3. Estimation of the Maximum Convective Wind Gust

3.1 *Buoyancy*

As in Emanuel [12], the downdraft convective available potential energy is defined as:

$$\mathrm{DCAPE} \equiv U_{\mathrm{BUOY}} = \int_{p_H}^{p_S} R_d \left[T_\rho^{(\mathrm{ambient})} - T_\rho^{(\mathrm{parcel})} \right] d\ln p \qquad (3)$$

In Eq.(3), p is atmospheric pressure, R_d the gas constant of dry air and T_ρ the density temperature of a moist and

Corresponding address: Linus H.Y. Yeung, Hong Kong Observatory
E-mail address: hyyeung@hko.gov.hk.

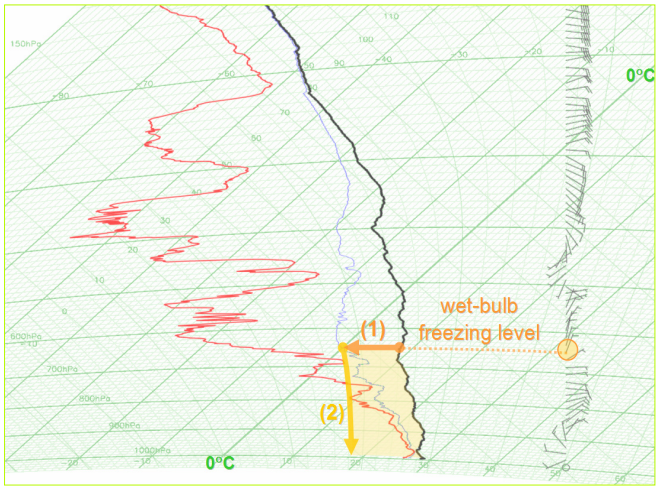

Fig. 2 Two-stage thermodynamic processes of downdraft — (1) isobaric cooling by evaporation of raindrops; (2) pseudo-adiabatic descent if favourable (i.e. inequality (2) satisfied). The shaded area represents DCAPE and is positive (negatively buoyant) in this illustration. The black, blue and red traces on the tephigram represent dry-bulb, wet-bulb and dew-point temperatures respectively.

cloudy parcel. T_ρ is very similar to virtual temperature T_v but with the effect of rain water and cloud ice included. In practice, the mixing ratios of those two hydrometeors are not directly observed and are usually several orders of magnitude smaller than the mixing ratio of water vapour. As such, T_ρ is approximated by virtual temperature T_v, data of which are readily retrievable from radiosonde measurements.

To calculate the integral in Eq.(3) directly, the downdraft height H or pressure level p_H has to be determined. To this end, the theoretical view of Emanuel [12] is adopted, namely the maximum potential energy achievable by a parcel is realized by a two-stage process: (i) isobaric cooling through a wet-bulb process; (ii) descending along a pseudo-adiabat to the ground, with just enough evaporation to keep the parcel saturated. This 2-stage process is illustrated in Fig. 2 using the tephigram and the yellowish shaded area shown gives U_{BUOY}. It is positive if the net buoyancy force is pointing downward and negative if the net buoyancy force is pointing upward. For neutral buoyancy, $U_{\text{BUOY}} = 0$.

Following Nakamura [7], it is further assumed that the downdraft originates near the melting level for precipitation, i.e. the wet-bulb freezing level. This choice of downdraft height is justified in the sense that the altitude is low (warm) enough for evaporative cooling to be efficient and yet high (cold) enough for an upper bound on DCAPE to be estimated.

3.2 *Precipitation Loading*

Following Emanuel [2], Wolfson [5] and Doswell [10], the force of precipitation loading on an air parcel is parameterized as:

$$L = -g \cdot r_\ell$$

where r_ℓ is the liquid water mixing ratio and g the acceleration due to gravity. The total gravitational potential energy due to water loading is obtained by integrating over the downdraft column [11]:

$$U_{\text{LOAD}} = -2\int_0^H L\,dz = 2g\int_0^H r_\ell\,dz\,. \qquad (4)$$

When the integrand is multiplied by the mean density $\overline{\rho}$ of the downdraft air column, the resulting integral becomes the vertically integrated liquid (VIL) water, which is readily available from radar observations. Following Holleman [11], the mean density is approximated by using a standard atmosphere in the lowest 5 km and the gravitational potential energy term becomes simply

$$U_{\text{LOAD}} = 20.3 \times \text{VIL}\,. \qquad (5)$$

Here, VIL is in unit of kg/m^2 and the proportionality constant in (m/s)^2/(kg/m^2). By rewriting the unit of VIL as

$$\text{kg}\cdot\text{m}^{-2} = \text{m}\cdot\text{kg}\cdot\text{m}^{-3} = \text{mm}\cdot(1000\,\text{kg}\cdot\text{m}^{-3})$$

and noting that water density is approximately 1,000 kg/m^3, VIL can also be expressed more conveniently in terms of mm of rainfall per unit area.

3.3 *Initial Parcel Momentum*

As a parcel descends from the wet-bulb freezing level, its initial momentum v_H aloft is assumed to be transferred down to the surface without major modification. Assuming also that the initial vertical motion of the parcel is insignificant, v_H can then be approximated by the horizontal wind speed at the wet-bulb freezing level obtained from radiosonde measurements.

4. Development of a Squalls Nowcasting Algorithm

4.1 *Data Sets*

Thunderstorm cases in 2000-2006 with reported severe squalls at 70 km/h or higher were selected as the basic data set in developing the nowcasting algorithm. The cases were further divided into two groups, namely 2000-2003 and 2004-2006, as the training and test data sets respectively.

Examination of the 1-sec wind gust measured by various automatic weather stations (AWS) over Hong Kong showed that the gust factors at higher altitudes differed significantly from those observed near the ground level. To avoid introducing complicating factors into the present downburst conceptual model, only station data at altitudes below 200 m were included in the AWS data set. This left us with a total of 25 severe squalls cases, 15 in the training subset and 10 in the test subset. When there were multiple stations reporting severe gusts, the highest record was used to validate the corresponding squalls nowcast.

For each observed squall event, nowcast data were generated every 6 minutes over an extended time period covering the actual occurrence time of the squalls. For the 25 historical severe squalls events, a total of 1,015 nowcasts were generated, with 630 in the training set and 385 in the test set.

4.2 *Use of Radar Data*

The estimation of the maximum possible wind gust was performed using the method outlined in Section 3. H, v_H and U_{BUOY} were all calculated from the latest ascent data available at forecast time. For U_{LOAD}, the required VIL data were generated from a mosaic of two S-band Doppler weather radars in Hong Kong, located at Tai Mo Shan (TMS) and Tate's Cairn (TCR) (Fig. 3). The characteristic of the two radars are very similar with volume scans updated very 6

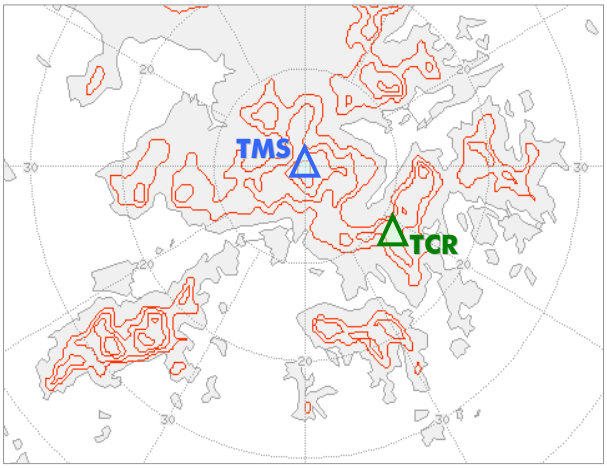

Fig. 3 Locations of the two S-band Doppler weather radars in Hong Kong. Tai Mo Shan (TMS) and Tate's Cairn (TCR) radars are marked by triangles in blue and green respectively. Also shown on the map are height contours at 200 m separations and concentric rings at 10 km spacing. The distance between the two radars is around 11 km.

minutes in synchronization.

In theory, the VIL required in Eq.(5) or the integral in Eq.(4) should be summed from the ground level to the downdraft origin height H. In practice, H was determined from 12-houly ascent data, hence limiting its accuracy especially during rapidly changing situations. Moreover, the altitude of the TMS radar is about 950 m, below which there is no radar observation. As a compromise, the integration in Eq.(4) was restricted to 1-5 km only. Furthermore, it was considered that the rain core would be the most effective part insofar as precipitation loading is concerned. In other words, the most intense VIL pixels pertaining to each detected downburst cell were expected to dominate in the calculation of the corresponding gust contribution. Empirically, the VIL data input to Eq.(5) was estimated by taking the average value of the top 25 % VIL pixel values.

As mentioned in Section 2, a downdraft is triggered by precipitation but obviously not all rainfall events trigger a significant downdraft. By examining the squall cases in the training data set, a minimum of 5 mm was adopted for VIL in screening out thunderstorm cells with little or nil potential of developing downburst. It is interesting to note that the 5-mm VIL threshold implies a velocity equivalent of $\sqrt{20.3 \times 5}$ ≈ 10 m/s (by taking square root of Eq.(5)), precisely one third contribution to a gust wind at gale force (≈ 17.5 m/s; and note that $\sqrt{17.5^2 / 3}$ ≈ 10 m/s). The above VIL threshold value is considered a reasonable choice for severe wind gust prediction, assuming the three contributions to convective gust in our conceptual model are of similar order of magnitude.

4.3 *Nowcast Strategy, Definitions and Simplifications*

With the criterion on precipitation strength (the 5-mm VIL threshold) and the implicit requirement on rain area (including only the top 25% of VIL pixels in a storm cell) as described in detail in Section 4.2 above, the inequality (3) introduced in Section 2 becomes more restrictive and sets a criterion on the potential energy required for triggering a significant downdraft over a localized area. In the present nowcasting

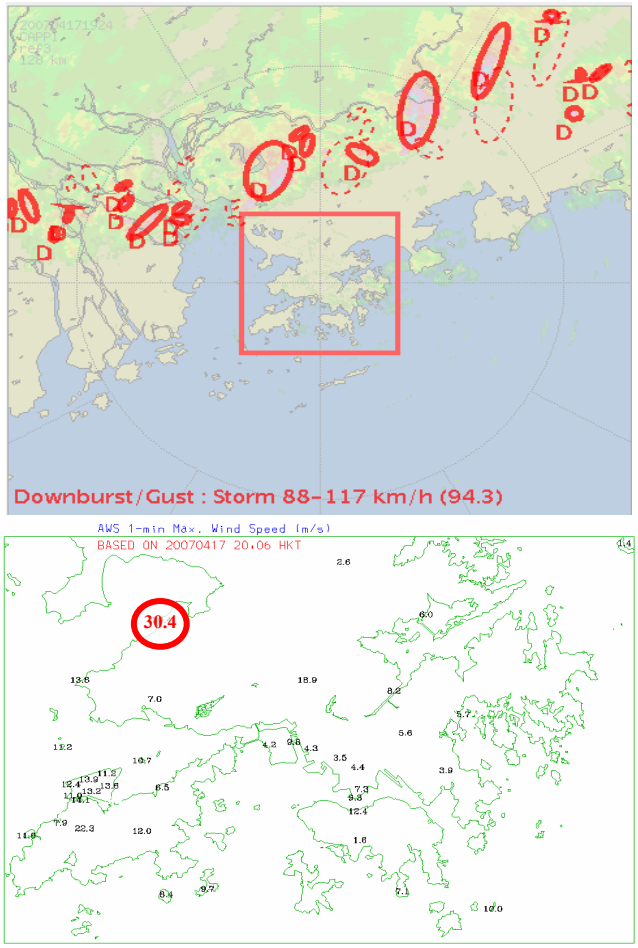

Fig. 4 Squall line on 17 April 2007. Upper panel shows the first severe downburst/squalls alert message (94.3 km/h or 26.7 m/s) issued at 7:24 pm. (Plot convention: red ellipses tagged with letter "D" represent downburst/squalls threat areas; dashed ellipses represent forecast positions at 30 min lead time; warning zone of Hong Kong is bounded by red lines. Also shown on the background is the map of Hong Kong and neighbouring regions, overlaid with 3-km reflectivity map.) Lower panel displays the 1-min maximum wind speed (i.e. the maximum of sixty 1-sec wind gust records) at 8:06 pm when severe gust (30.4 m/s) was first detected in Hong Kong at the AWS encircled in red.

scheme, downburst is defined in such a context. Once triggered, the predicted severity of a downburst is defined by its maximum possible convective gust achievable at the surface and is calculated using Eq.(1).

To analyze the correlation between the predicted downbursts or squalls and the observed gusts, two simplifications were made: (i) each detected downburst cell is represented by an ellipse (computed by standard principal component transformation method); (ii) the elliptic area constitutes a downburst/squalls threat area. Due to the hilly terrain in Hong Kong (see also Fig. 3) and the scarcity of surface observations over the surrounding waters, the actual propagation speed and pattern of a gust front approaching or traversing over the land mass were largely ignored in the representation of squalls threat.

For similar reasons, it would be difficult to associate unambiguously a severe squalls event detected on the ground with specific downburst cells aloft. Instead, the correctness of a downburst/squalls nowcast was quantified by checking its

threat area against a warning zone (~ 64×64 km^2 in area) of Hong Kong (illustrated in the top panel of Fig. 4). If a threat area came into the warning zone, the corresponding nowcast was counted as a "yes" prediction. If multiple downburst cells existed, their totality constituted a threat area. Amongst such downburst cells, the highest predicted gust was selected for generating the corresponding alerting message (the red text below the warning zone in the top panel of Fig. 4) and compared against the highest gust recorded in the next 30 minutes by AWS.

To ensure a higher correlation between a prediction and a recorded gust during algorithm development, a relatively short time window of 30 minutes was imposed. For the verification of real-time forecasts (see Section 5 below), such a restriction was relaxed to allow for more possibilities, e.g. very persistent downburst cells embedded in a squall line.

4.4 *Test Results and Parameter Tuning*

Fig. 5 showed the test results before and after tuning. As indicated by the blue circles in Fig. 5, the maximum convective wind gust computed directly from Eq.(1) is excessively over-predicted. Examination of the contributions from individual terms in Eq.(1) revealed that the high bias stemmed from an over-estimation of DCAPE, with velocity equivalent often exceeding 38 m/s (about 37 % of all nowcasts) found in the training data set. Compared with the highest record of 37.6 m/s (hurricane force) found in the entire 2000-2006 data set, the direct estimation of gust contribution due to buoyancy acceleration using Eq.(3) was considered unrealistic.

As pointed out by Doswell [10] and Emanuel [12], there were various reasons for incomplete conversion of downdraft convective available potential energy into kinetic energy of gust winds, including non-continuous rainfall evaporation during parcel descent (such that the parcel warmed at dry adiabatic lapse rate and quickly lost its negative buoyancy), dilution of buoyancy and momentum through mixing with environmental air, as well as adverse perturbation pressure gradient acting upward. In their numerical simulation study of a rotating downburst, Parsons and Weisman [13] also reported that sharp descent of an air parcel was associated with large negative buoyancy, but such buoyancy was opposed by a strong upwardly directed dynamic pressure force as the parcel approached the surface.

To account for such unknown factors in the potential-kinetic energy conversion, we took on an empirical approach. We proposed a simple parameterization in which the actual contribution to wind gust by buoyancy force was capped by some maximum speed $v_{\max}$. By maximizing the forecast skill (critical success index or CSI was chosen) using the training data set, the optimal value of $v_{\max}$ was found to be about 12 m/s. The parameterized algorithm was validated against the test data set and similar skill level was achieved (CSI ~ 68 %). The squalls predictions after such a tuning were plotted as red circles in Fig. 5. For predicted squalls exceeding the severe gust threshold of 19.44 m/s, the mean and root-mean-square errors in the test data set were found to be 2.2 and 5.9 m/s respectively.

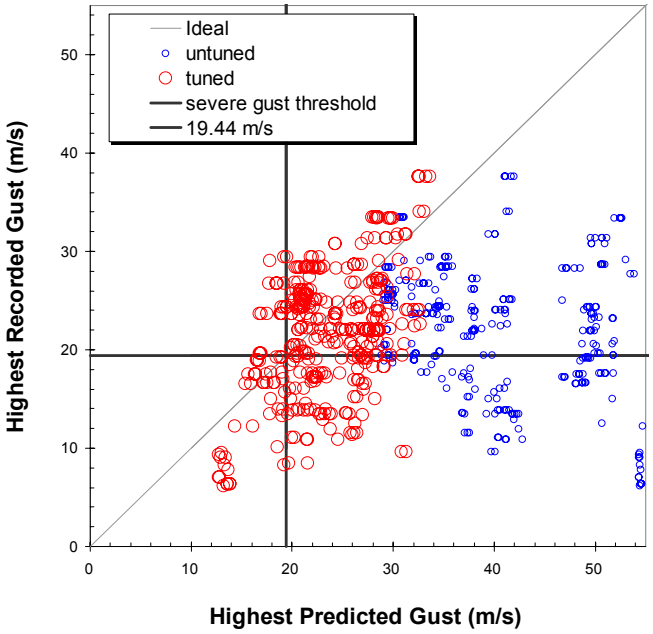

Fig. 5 Scatter plot showing highest recorded gust versus the predicted maximum convective gust in the test data set. Blue and red circles represent respectively predictions before and after tuning.

5. Real-time Trials

The downburst/squalls nowcasting algorithm has been put into real-time trial run in Hong Kong since April 2007. A forecast component was included in the algorithm by extrapolating the analyzed position and motion of a downburst cell out to 30 minutes. The concept of downburst/squalls threat area was expanded accordingly to include the forecast track.

Fig. 4 showed a squall line case in Hong Kong on 17 April 2007. The upper panel displayed the first severe squalls alerting message issued at 7:24 pm. In subsequent radar updates, alert messages were consistently issued with a peak gust prediction of 27 m/s (or 97.2 km/h, in storm force category) issued at 7:48 pm. The lower panel plotted the gust (viz "1-min Max. Wind Speed" in Fig. 4) data recorded at 8:06 pm when severe gust was first detected at an AWS (encircled in red) located over the northwestern coast of Hong Kong. The highest gust during the passage of the squall line was 31.6 m/s (also in storm force category), recorded at 8:19 pm at another location. In summary, the highest squalls, predicted or observed, in this particular case were in the same force category with a forecast lead time of about 42 minutes.

The overall performance of the algorithm was assessed quantitatively by verifying (event-based) the real-time nowcast data for all thunderstorm cases in 2007. Preliminary results indicated that the algorithm was able to score a probability of detection (POD) of about 80 %, with an average lead time about 30 minutes. Such good performance was achieved at a mean error of about 5.5 m/s and a false alarm ratio (FAR) of about 84%. Despite the relatively high FAR, the downburst/ squalls nowcast product was popular among forecasters for its high POD and the sufficiently long lead time for making warning decisions.

6. Discussion

Despite some initial successes, there are major limitations inherent in the present downburst/squalls nowcasting approach. First of all, severe squalls due to or in combination with other mechanisms, e.g. turbulence, may not be handled adequately. Secondly, the simplification to an ellipse is likely to lead to an under-estimation of the downburst/squalls threat area because the actual propagation of outflow or gust front can spread further downstream. Thirdly, there are still significant errors in the estimated maximum convective wind gust even after parameterization. One reason for the over-prediction bias seen in the test results (Section 4.4 refers) is the way the basic data set has been assembled with in-built bias towards historical gust events. For this reason, in routine real-time application, the FAR is likely to be even higher. Before the systematic errors can be reduced, the predicted squalls are perhaps best presented as category forecasts. In designing the graphical user interface, the squalls nowcast is actually presented in terms of wind force (see the top panel in Fig. 4) and issuance criterion of the alerting message is lowered to 17.5 m/s (gale force).

Within the current algorithm settings, there are still rooms for further enhancement through improving the observation data. At this stage, the algorithm relies heavily on radiosonde data launched only twice a day at 00 and 12 UTC. From a nowcasting perspective, more frequently updated upper-air data, e.g. wind profiler, are desirable.

The potential benefit of wind profiler data is explored by re-visiting the squall line case of 17 April 2007. The 00-UTC (8 am) upper-air wind observations near the wet-bulb freezing level were actually unavailable due to some instrumental problems. By default, the initial momentum of the downburst was estimated to be 17.8 m/s by interpolating wind reports at the nearest two levels. The contribution from precipitation loading as estimated from VIL data (at 7:48 pm) was about 16.3 m/s. Analysis using the corresponding tephigram (not shown) showed that a parcel at the wet-bulb freezing level would be negatively buoyant (positive area) and the DCAPE contribution was determined to be $v_{\max}$ (viz 12 m/s; c.f. direct estimation of 42.1 m/s using Eq.(3)!). Comparing the magnitudes of these three velocity estimates, the initial parcel momentum was the dominant factor in this case.

In hindsight, wind profiler data prior to the occurrence of the severe squalls actually revealed a wind speed of about 23 m/s (45 knots) near the freezing level. Ascent data obtained later at 12 UTC (8 pm) also indicated wind speed of similar magnitude. With such updated information ingested to estimate the dominant gust contribution, the maximum possible convective gust estimation for this case would have become 30.7 m/s, in closer agreement with the observed peak gust (31.6 m/s).

7. Concluding Remarks

Starting from a conceptual convective downdraft model, a radar/radiosonde-based algorithm was developed and presented as a viable objective tool for nowcasting severe squalls associated with thunderstorms. Alerts on the maximum possible convective wind gust likely to be induced near the ground level in Hong Kong was demonstrated to be operationally useful. Forecasters on the bench found that the new nowcasting tool could provide sufficient lead times for them to make timely warning decisions.

Research results based on historical squall events in 2000-2006 and real-time trial of gust cases in 2007 indicated that not only was the physically based approach capable of capturing the occurrence of convective squalls, but it could also delineate objectively the relative weights of the key physical processes involved, shedding light on the possible major error sources in gust estimation.

To further enhance the effectiveness of the squalls nowcasting algorithm, one potential improvement strategy is to use more frequently updated upper-air data. Along this line, wind profiler data with suitable treatments can be studied further as supplement or substitute for radiosonde wind observations. To extract more comprehensive upper-air thermodynamic information as input data, use of analyzed fields from rapidly-updated high-resolution NWP models can also be explored.

Acknowledgment

The authors would like to thank Mr H.G. Wai and Mr C.Y. Lam for their valuable comments on the manuscripts.

References

[1] Squires, P., 1958: "Penetrative downdrafts in cumuli", *Tellus*, vol. 10, pp. 381-389.

[2] Emanuel, K.A., 1981: "A similarity theory for unsaturated downdrafts within clouds", *J. Atmos. Sci.*, vol. 38, pp. 1541-1557.

[3] Stewart, S.R., 1991: "The prediction of pulse-type thunderstorm gusts using vertically integrated liquid water content (VIL) and the cloud top penetrative downdraft mechanism", Technical Memorandum, NWS SR-136, NOAA.

[4] Ivens, A.A.M., 1987: "Forecasting the maximum wind velocity in squalls", ESASP-282, Proc. Symp. Mesoscale Analysis and Forecasting, Vancouver, Canada, 17-19 August, 1987, ESA, pp. 685-686.

[5] Wolfson, M.M., 1990: "Understanding and predicting microburst", Preprints, 16th Conference on Severe Local Storms, Kananaskis Park, Alta., Canada, Amer. Meteor. Soc., pp. 340-351.

[6] McCann, D.W., 1994: "Windex — a new index for forecasting microburst potential", *Wea. and Forecasting*, vol. 9, pp. 532-541.

[7] Nakamura, K., R. Kershaw and N. Gait, 1996: "Prediction of near-surface gusts generated by deep convection", *Meteor. Appl.*, vol. 3, pp. 157-167.

[8] Hand, W.H., 2000: "An investigation into the Nimrod convective gust algorithm". Forecasting Research Technical Report, No. 321, UK Met Office.

[9] Geerts, B., 2001: "Estimating downburst-related maximum surface wind speeds by means of proximity soundings in New South Wales, Australia", *Wea. Forecasting*, vol. 16, pp. 261-269.

[10] Doswell, C.A., 1993: "Extreme Convective Windstorms: current understanding and research", Proceedings of Spain-U.S. Joint Workshop on Natural Hazards, Barcelona, Spain, 8-11 June 1993.

[11] Holleman, I., 2001: "Estimation of the maximum velocity of convective wind gusts", Internal Report, KNMI IR-2001-02, KNMI.

[12] Emanuel, K.A., 1994: *Atmospheric Convection*, Oxford University Press, 1994, pp. 171-173.

[13] Parsons, D.B. and M.L. Weisman, 1993: "A numerical study of a rotating downburst", *J. Atmos. Sci.*, vol. 50, pp. 2369-2385.